

Grand Unification II: Hot Accretion and AGN Jets

Renyue Cen¹

Received _____; accepted _____

¹Princeton University Observatory, Princeton University, Princeton, NJ 08544;
cen@astro.princeton.edu

ABSTRACT

We show that a quasi-spherical (QS) hot accretion flow is expected to operate in all SMBHs, with its rate being capped at $\dot{m}_{QS,max} \sim 0.001(M/10^8 M_\odot)$ in units of the Eddington rate. It is then proposed that AGN jet power is proportional to the product of the hot accretion rate and a SMBH spin-dependent efficiency for energy extraction in the form of jets. Predictions from this model include (1) while radio jets should emerge from all SMBHs, the maximum jet power goes with SMBH mass approximately as $10^{43.6}(M/10^8 M_\odot)^2$ erg/s, (2) even although there are two separate underlying populations of radio-quiet (RQ) and radio-loud (RL) AGNs, any bimodality in the observed AGN radio loudness distribution is likely due to a selection effect, such as some imposed optical magnitude limits, (3) the RL fraction of quasars is expected to decrease with redshift in the cold dark matter model, (4) host galaxies of RQ and RL quasars should be drawn from the same underlying elliptical galaxy population, although RL quasars may have SMBHs that are somewhat more massive than their RQ counterparts and RL quasars may reside predominantly in core elliptical galaxies, (5) RL low-luminosity AGNs and LINERs may represent the long, declining “trailing” phase following the initial, more luminous AGN phase, (6) a broad anti-correlation between radio-loudness and disk accretion rate is expected, (7) RL AGNs may be expected to be more abundant in Type Ia supernovae than RQ AGNs, (8) among RL AGNs a correlation between radio power and clustering strength is predicted, and (9) RQ and RL AGNs should have, on average, similar IR-optical-UV properties.

Subject headings: black hole physics - galaxies: active - galaxies: bulges - galaxies: interactions - radio continuum: galaxies - quasars: general

1. Introduction

The past decades have witnessed a tremendous amount of effort devoted to understanding the observed complexities of AGNs. This pursuit of intrinsic simplicity has been remarkably fruitful. The most successful unification scheme hinges on a simple assumption that the observed optical/UV properties of an AGN depends only on the relative orientation of the observer’s line of sight to the non-spherical configuration of the central engine, which is believed to be composed of a SMBH (Rees 1984), an optically thick and geometrically thin accretion disk, a surrounding hot corona, an obscuring torus of gas and dust (Antonucci 1993) and a diverse set of gas clouds moving at a variety of speeds at different locations (e.g., Elvis 2000). Unification proposals among RL AGNs, based on viewing orientation dependent Doppler effect of the relativistic (twin) radio jets, also enjoy great successes (Barthel 1989; Urry & Padovani 1995).

The observational fact that most of, and perhaps all, non-active, bulged galaxies harbor SMBHs at their centers (e.g., Richstone et al. 1998) and the existence of a tight correlation between the observed central SMBH mass and bulge stellar mass (or velocity dispersion) (e.g., Magorrian et al. 1998; Ferrarese & Merritt 2000; Gebhardt et al. 2000; Merritt & Ferrarese 2001; Tremaine et al. 2002) strongly suggest that growth of SMBHs and formation of galaxies, in particular, the galactic spheroid component, are intricately linked (e.g., Haehnelt, Natarajan, & Rees 1998). Motivated by these strong observational indications, we intend to embark on, through a series of focused papers, a coherent physical framework for coupled formation and evolution of galaxies and AGNs, in hopes of ultimately helping build a grand unification theory. Earlier attempts along this direction are typified by the pioneering work of Kauffmann & Haehnelt (2000), based on plausible but heuristic assumptions on coupled formation of galaxies and AGNs. In the first paper of this series (Cen 2006), we put forth a more physically provoking explanation for the observed SMBH

mass-bulge velocity dispersion relation, in the context of hierarchical structure formation model. This paper is the second of the series. We show a co-existence of two accretion (hot and cold) modes on SMBH scales and propose that the hot accretion, in conjunction with the spin of the SMBH, determines the AGN jet power. In §2 we present a theory on the dependence of hot accretion rate and the jet power on the mass of the SMBH. In §3 some observational tests and predictions are made, followed by conclusions in §4.

2. Hot Accretion and AGN Jet Power: Theory

2.1. Basic Assumptions and Maximum Hot Accretion Rate

We are interested in knowing the state of hot gas on its way to the SMBH. For ensuing derivations, we utilize the observed SMBH mass (M)-bulge (1-d) velocity dispersion (σ) relation (Tremaine et al. 2002):

$$M = 10^{8.13} \left(\frac{\sigma}{200 \text{ km s}^{-1}} \right)^4 M_{\odot}. \quad (1)$$

Cen (2006), in a specific model, showed that this relation may not evolve with redshift. Assuming that the gas temperature T relates to σ by $kT/\mu = m_p \sigma^2$, where $\mu = 0.58$ is the molecular weight, m_p the proton mass and k the Boltzmann constant, we obtain (with specific heat $\gamma = 5/3$)

$$r_B = 14.9 \left(\frac{M}{10^8 M_{\odot}} \right)^{1/2} \text{ pc}. \quad (2)$$

With Equations (1,2) and the adopted temperature-velocity dispersion relation we can further relate the gas density at r_B , n_B , to the (adiabatic) Bondi (1952) accretion rate, \dot{m}_B , in Eddington units (\dot{M}_E), as a function of M :

$$n_B = 2.7 \times 10^3 \dot{m}_B \left(\frac{M}{10^8 M_{\odot}} \right)^{-1/4} \text{ cm}^{-3}, \quad (3)$$

where $\dot{M}_E \equiv 2.2(M/10^8 M_\odot) M_\odot/\text{yr}$ is the Eddington rate. Equation (3) provides a way to relate hot gas cooling time to the accretion rate for a fixed SMBH mass. In what follows all accretion rates are expressed in the Eddington rate.

We distinguish a hot, quasi-spherical Bondi accretion mode of rate \dot{m}_{QS} from a cold disk accretion mode. While the cold disk accretion mode of rate, $\dot{m}_d = \dot{m}_{hc} + \dot{m}_c$, consist of two components, one of rate \dot{m}_{hc} from cooling of a hot component en-route from galactic scales to the SMBH and the other of rate \dot{m}_c from direct infall of cold gas from galactic scales, \dot{m}_{QS} comes solely from direct infall of hot gas from galactic scales that remains in the hot component when reaching the SMBH. Suppose that the hot gas would have had an accretion of rate \dot{m}_h feeding the SMBH, if it did not cool. But when the hot gas cools through its way to the SMBH scale from galactic scales, \dot{m}_h will be split into \dot{m}_{QS} and \dot{m}_{hc} . We are interested in computing \dot{m}_{QS} here.

First, a qualitative consideration. Assuming, conservatively, the no-outflow case where hot gas density scales with radius as $\rho(r) \propto r^{-3/2}$ and that the hot gas is at the virial temperature in the radial range $r < r_B$, then, it can be shown that the ratio of gas cooling time to dynamical time is $t_{cool}/t_{dyn} \propto T/\Lambda(T)$, where $\Lambda(T)$ is the volumetric cooling function. Since $\Lambda(T) \propto T^\gamma$ with $\gamma < 1$ ($\gamma \sim 0.5$ for $T > 10^7 \text{K}$ with bremsstrahlung cooling) for the temperature range of interest here, t_{cool}/t_{dyn} is an increasing function of decreasing radius from the SMBH in the radial range $r < r_B$. On the other hand, in the radial range $r > r_B$ where rotation curve is nearly flat (Sofue & Rubin 2001; Gavazzi et al. 2007), assuming that infalling gas density goes as $r^{-\gamma}$, then, as long as γ is greater than 1, the ratio t_{cool}/t_{dyn} decreases with decreasing radius, reaching a minimum at r_B . As we have argued in Cen (2006), γ is likely close to 2. The above two considerations indicate that t_{cool}/t_{dyn} has a minimum at r_B . Thus, one may estimate, probably to within a factor of a few, the amount of hot gas that will ultimately feed the SMBH, using physical arguments based on

the ratio t_{cool}/t_{dyn} at r_B . Guided by this, let us denote a critical hot QS-Bondi accretion rate as \dot{m}_0 , at which $t_{cool}/t_{dyn} = 1$ at r_B . We use the cooling function from Sutherland & Dopita (1993), assuming solar metallicity for the hot gas.

Let us now make a more quantitative calculation. There are two separate regimes in the hot accretion rate space. For $\dot{m}_h \ll \dot{m}_0$, almost the entire hot gas accretion rate \dot{m}_h may be expected to ultimately feed the SMBH in *hot* flow. In the other regime where \dot{m}_h is not much smaller than \dot{m}_0 , a progressively larger fraction of the hot gas will cool and “drop out” to fall onto the accretion disk to (potentially) feed the SMBH in *cold* flow or form stars. Under the assumptions (1) that the fraction of hot gas that “drops out” to become cold gas at each radius is directly proportional to the net cooling rate, (2) that already cooled gas does not get heated back up to return to the hot phase (i.e., assuming gas is thermally unstable, once being cooled) and (3) that the (remaining) hot gas is at the virial temperature at each radius, then, we may write the evolution equation for the hot gas:

$$\frac{d(\rho_r r^2 v_r)}{dr} = \frac{2\mu \rho_r^2 r^2 \Lambda(T_r)}{3k T_r m_p} - \frac{4\mu m_p r \rho_r \sigma_r^2 v_r}{3k T_r} - r \rho_r v_r \frac{d \ln T_r}{d \ln r} - \frac{\mu m_p r \rho v_r^3}{3k_r T} \frac{d \ln v_r^2}{d \ln r}, \quad (4)$$

where r is the SMBH-centric radius, ρ_r , v_r , σ_r and T_r are the hot gas density, radial velocity, velocity dispersion and temperature at r , respectively. The first term on the right hand side of Equation (4) is the hot gas drop-out rate due to radiative cooling and the second term due to heating by the total gravitational energy released, with some of the released gravitational energy going to heat up the (remaining) hot gas to the virial temperature (the third term) and to accelerate the radial velocity (the fourth term). Let us define $x \equiv r/r_B$ and $y \equiv (\rho/\rho_0)(r^2/r_B^2)(v_r/v_B)$, where ρ_0 is the gas density at r_B that corresponds to the critical accretion rate of \dot{m}_0 , v_B is the radial velocity at r_B . Note that y is a “normalized” mass flux for the hot flow and would be constant in the absence of gas “drop-out”. In Equation (4) we still need to specify v_r , which normally can be obtained by solving the radial velocity equation under the combined gravity and pressure force. But

here we will take a somewhat different approach by taking into account “non-spherical” components in our spherical Equation (4), to be consistent with our Assumption (3) above. That is, we require some viscous processes to turn radial kinetic energy into thermal energy, which, for example, may be accommodated by internal shocks in each radial shell. Hence, in conjunction with Assumption (3), we make one further simplifying Assumption (4) that $v_r = \sigma_r$, where v_r may be considered as an “assemble” radial velocity at r . In other words, some extra counteracting pressure force will be generated, if gas motion becomes supersonic. We note that the combination of Assumptions (3,4) precisely conserves energy in a Keplerian potential, which in our case corresponds to the radial range $r \leq r_B$ that primarily determines the final hot accretion rate (see below). However, it is noted that, if a different assumption, say, $v_r = 0.5\sigma_r$, is made, the results only change $\sim 20\%$.

Thus, finally, we obtain a simplified hot gas evolution equation:

$$\frac{dy}{dx} = \frac{1.4y^2}{x^2} \frac{\Lambda(T_x)T_B v_B^2}{\Lambda(T_B)T_x v_x^2} - \frac{4y}{3x} - \frac{4y}{3x} \frac{d \ln T_x}{d \ln x} \quad (5)$$

where $[\Lambda(T_x), \Lambda(T_B)]$, (T_x, T_B) and (v_x, v_B) are the volumetric cooling functions, temperatures and radial velocities at $(x, x = 1)$, respectively. In obtaining Equation (5) we have used the definition that $t_{cool}/t_{dyn} = 1$ at $x = 1$ for the hot accretion rate of \dot{m}_0 . The coefficient 1.4 reflects the difference between $(\rho/m_p)^2$ and $n_t n_e$ that is used in association with Λ , where n_t and n_e are the total volume density of ions and electrons, respectively.

Solving Equation (5) is a boundary condition problem. The outer boundary condition is provided by y_i , which corresponds to a hot gas density that would give a hot accretion rate of $y_i \dot{m}_0$, if the hot gas is not allowed to cool. For a given value of y_i , we integrate Equation (5) inward from some large x to $x = 0$ to obtain $y_f \equiv y(x = 0)$. To facilitate a more tractable calculation, we assume, reasonably, that at $r \geq r_B$ the rotation curve is flat and at $r < r_B$ the rotation curve is Keplerian. Figure 1 shows y_f as a function of y_i for five cases with $T_B = (10^{5.5}, 10^6, 10^{6.5}, 10^7, 10^{7.5})$ K, corresponding roughly to $M = 10^6 - 10^9 M_\odot$.

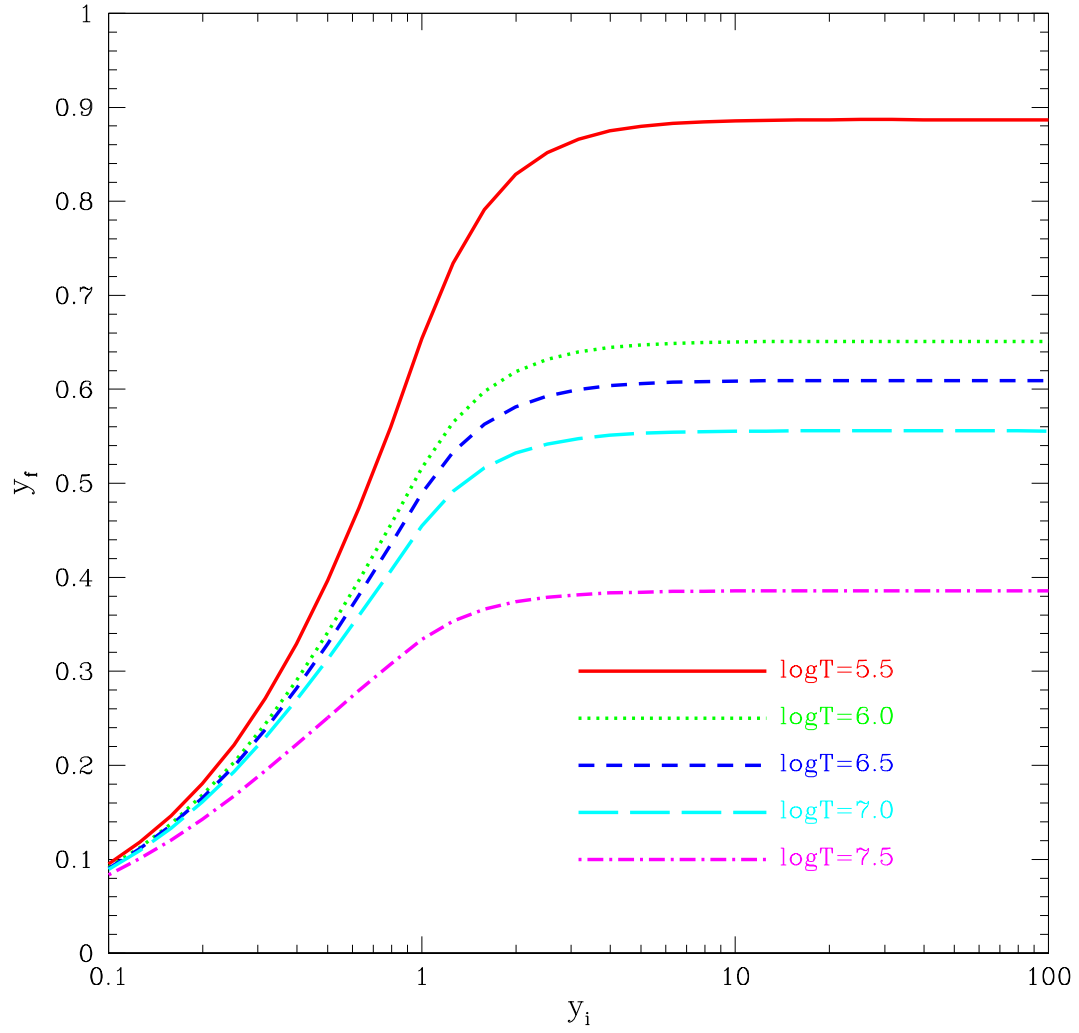


Fig. 1.— shows y_f as a function of initial y_i , computed based on Equation (5), for five cases with $T_B = (10^{5.5}, 10^6, 10^{6.5}, 10^7, 10^{7.5})$, with (solid, dotted, dashed, long-dashed, dotted-short-dashed) curves, respectively.

We find that, when $y_i \gg 1$, $y_f = 0.6 \pm 0.3$, for $T_B = 10^{5.5} - 10^{7.5}$ K. The relatively weak dependence of $\dot{m}_{QS,max}$ on T_B (hence SMBH mass) reflects features in the cooling function Λ . At $\dot{m}_h \leq 0.1\dot{m}_0$, practically all hot flow goes to the SMBH, as expected.

It is prudent to note that our spherical treatment would break down at some small radius, because the angular momentum of the hot accreting gas is finite and the hot accretion may significantly deviate from sphericity at some small radii. It is thus instructive to check where the gas “drop-out” from the hot flow practically stops. Figure 2 shows the evolution of y_x as a function of x with $y_i = 10^3$ (i.e., $\dot{m}_h = 10^3\dot{m}_0$) for two cases with $T_B = (10^{5.5}, 10^{7.5})$ K. We see that most of the drop-out occurs at large radii $x > 1$. Then, most of the remaining drop-out within Bondi radius (i.e., $x < 1$) occurs at $x > 0.1$. This indicates that hot gas drop-out in the high y_i limit ceases at quite a large radius, close to the Bondi radius, where the assumption of a hot spherical flow may be relatively good. For lower values of y_i , this would occur at still larger radii. Therefore, our computed rate \dot{m}_{QS} , while not exact, may be good to within a factor of order a few, which is adequate for our illustration. Figure 3 shows the computed maximum hot accretion rate onto the SMBH, $\dot{m}_{QS,max}$, as a function of M , with the following simple fitting formula accurate to within 30% for the SMBH mass range $M = 10^7 - 10^{9.5}$ M_\odot :

$$\dot{m}_{QS,max} = 0.001 \left(\frac{M}{10^8 M_\odot} \right), \quad (6)$$

shown as a dotted-long-dashed line in Figure 3.

Our essential point is that, in general, the gas accretion onto SMBHs is composed of two *concurrent* accretion modes and in particular the hot accretion flow of rate \dot{m}_{QS} exists at all times. We note that the idea of hot accretion flow around SMBHs is not new. Several well known classes of physical models have been proposed to understand the apparent radiative inefficiency of accretion onto some SMBHs at a low accretion rate: advection-dominated accretion flow (ADAF; Ichimaru 1977; Narayan & Yi 1994; Kato,

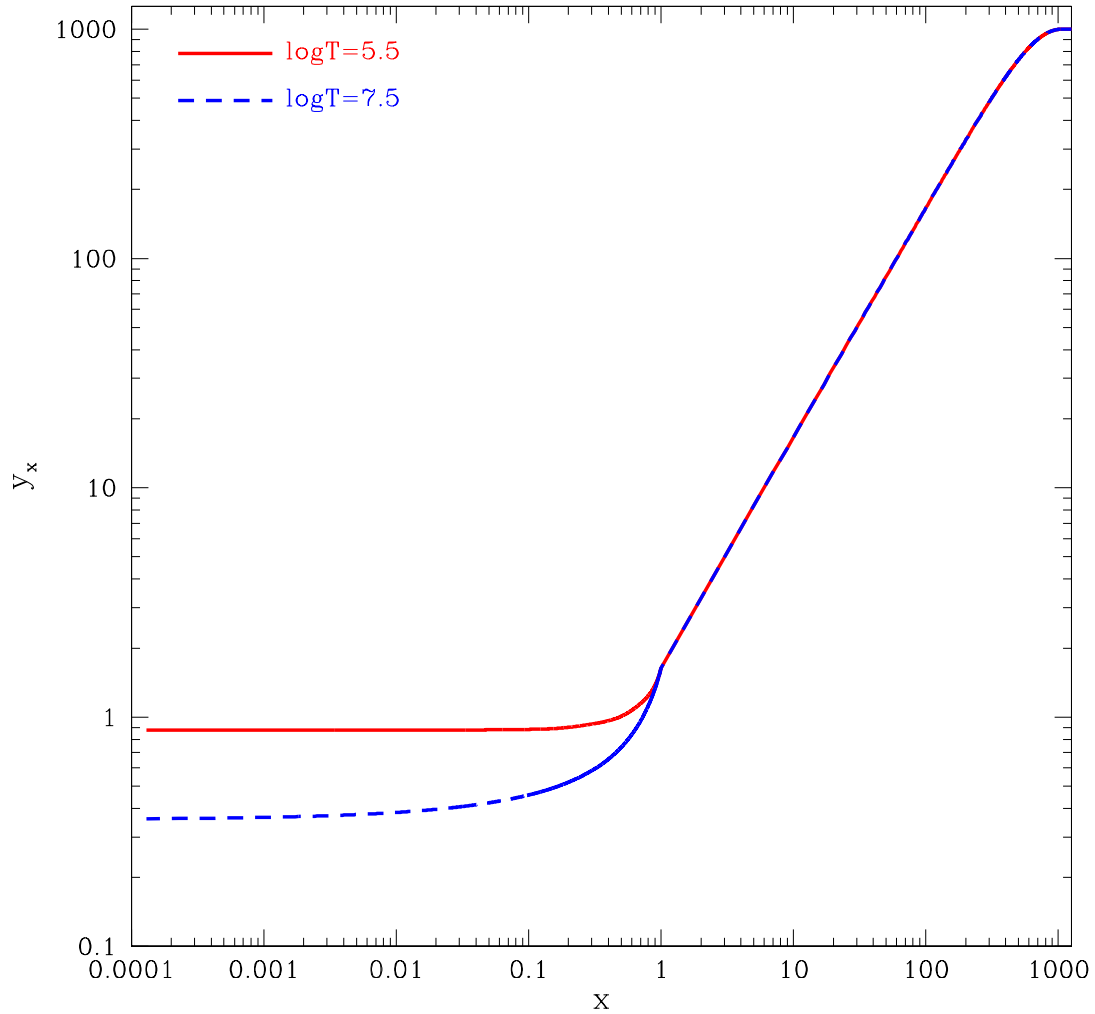


Fig. 2.— shows y_x as a function of initial x , for two cases with $T_B = (10^{5.5}, 10^7, 10^{7.5})$ and both with an initial $y_i = 10^3$ (i.e., $\dot{m}_h = 10^3 \dot{m}_0(M)$), with (solid, dashed) curves, respectively.

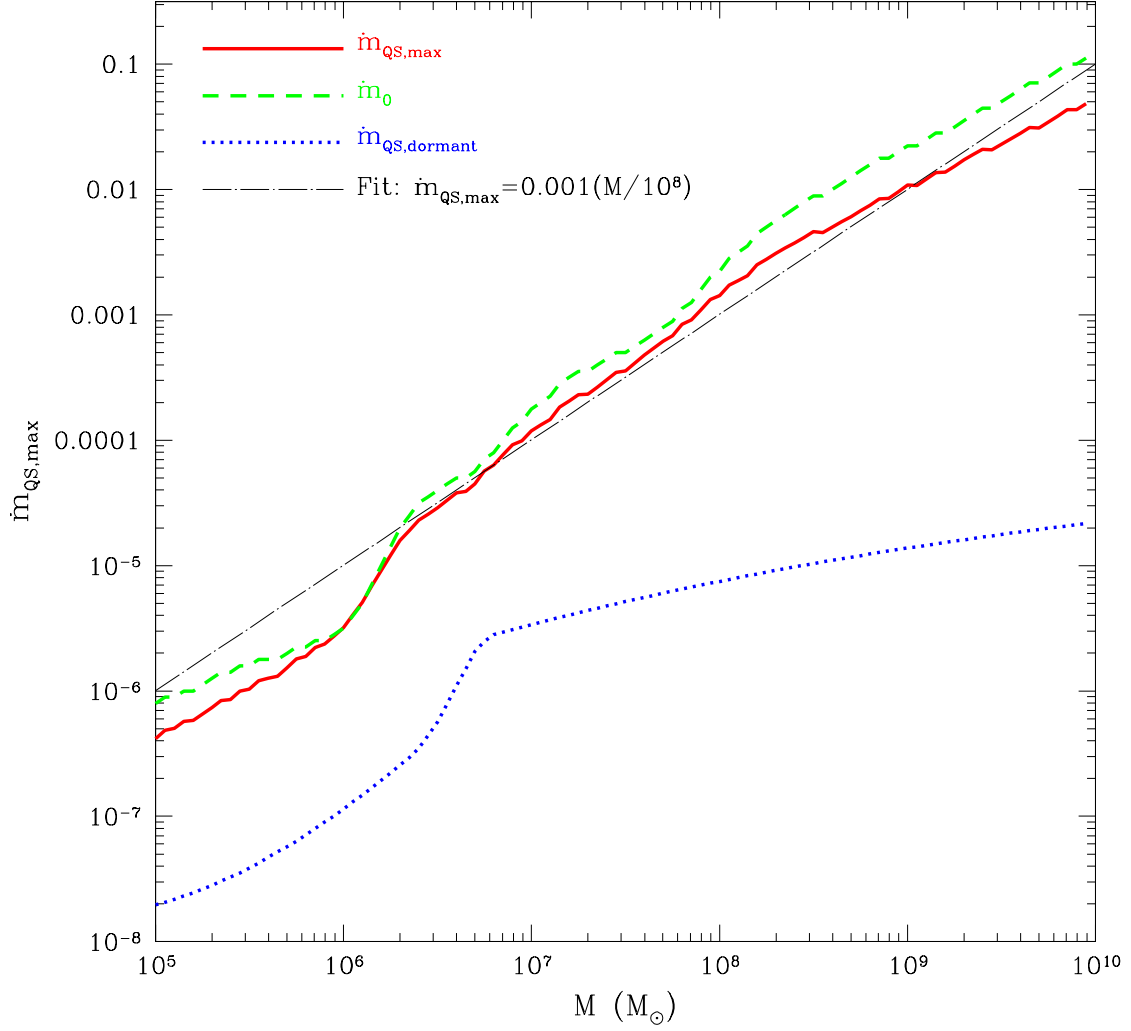


Fig. 3.— The solid and dashed curves show the maximum hot QS-Bondi accretion rate and \dot{m}_0 , respectively, in Eddington units as a function of M . The dotted curve shows the Bondi accretion rate in a “dormant” state. Also shown as dotted-long-dashed curve is a simple fitting formula, Equation (6)

Fukue, & Mineshige 1998), convection-dominated accretion flow (CDAF; Quataert & Gruzinov 2000) and an inflow-outflow variant (Blandford & Begelman 1999), among others. A mere extension proposed here is that one should expect a *co-existence* of a hot accretion even in the regime where the total accretion rate is high (i.e., $\gg \dot{m}_0$). The concept of a possible co-existence of different accretion modes near the SMBH has been put forth by Chakrabarti & Titarchuk (1995), where the shock-heating-produced hot gas within ten Schwarzschild radii was proposed for the primary purpose of Comptonization of disk emitted photons. We self-consistently compute the accretion rate of the hot component in a way that takes into account the en-route processes. More importantly, here, we point out that the mix of cold and hot flow, in particular, the maximum hot flow rate $\dot{m}_{QS,max}$, depends strongly on M , which may have profound ramifications with regard to AGN jet production, among others. We stress that, while the numerical values obtained by solving the simplified Equation (5) are certain to contain errors, the strong dependence of $\dot{m}_{QS,max}$ on M is primarily a result of the strong dependence of \dot{m}_0 on M (dashed curve in Figure 3) that does not rely on all the assumptions employed to arrive at Equation (5).

2.2. Hot Accretion Flow and AGN Jet Formation

Inflow hot gas to SMBHs is likely significantly pre-enriched with magnetic fluxes from earlier supernova remnants. Hence, realistic treatments of its dynamics would require explicit inclusion of magnetic field (e.g., Proga & Begelman 2003; Casse & Keppens 2004; Kato, Mineshige, & Shibata 2004; Proga 2005; De Villiers et al. 2005; McKinney 2005; Krolik, Hawley, & Hirose 2005; Hawley & Krolik 2006). An emerging feature from these studies of inflow gas of various initial configurations with the inclusion of magnetic field is the strong possibility of the production of bipolar magnetic jets and funnel outflows. The former are akin to the magnetic tower (Lynden-Bell 1996, 2003, 2006).

One primary discovery that is borne out from these simulations is that, without significant external thermal pressure with effectively a large “scale-height”, a magnetic tower fails to develop into a relativistic jet. The limited ability of magnetic self-confinement/collimation was previously known (e.g., Eichler 1993; Spruit, Foglizzo, & Stehle 1997; Okamoto 1999). We follow this indication and make the following critical *ansatz*: the QS-Bondi flow is responsible for the confinement and collimation of (twin) jets, by providing the requisite external pressure, and the strength (power) of the collimated jets is directly commensurate with the external pressure hence the QS-Bondi accretion rate. This conjecture could find its precedent in the seminal work of Rees et al. (1982), where an ion-pressure supported thick disk was proposed to collimate a pair of radio jets. We suggest here that the external pressure provided by the hot accretion can “naturally” act to collimate and power the jet, as simulations have begun to indicate. Another important discovery from relativistic MHD jet simulations (e.g., McKinney 2005; Hawley & Krolik 2006) is that the energy extraction efficiency, $\beta(a/M)$ (a is the spin of the SMBH), in the form of jet power in terms of accretion rate is a strong function of the spin of the central SMBH, in the vein of Blandford & Znajek (1977). Combining these ideas, we propose that the jet power goes as

$$P_{radio} = \beta(a/M) \dot{m}_{QS} \dot{M}_{Edd} c^2. \quad (7)$$

Recently, Allen et al. (2006) provide strong observational evidence that hot accretion may indeed be responsible for radio jet power in galaxies with moderate jet powers ($P_{jet} \sim 10^{41} - 10^{44}$ erg/s). While our proposed picture was conceived before that paper was submitted, these new observations provide an impetus. Further, Wilson & Colbert (1995) first made the suggestion that SMBH spin may be responsible for the dichotomy between RQ and RL AGNs, although their overall scenario differs from ours (see below). McKinney (2005) provides a fitting formula $\beta(a/M) = 0.07[\Omega_H/\Omega_H(a/M = 1)]^5$, where $\Omega_H = ac/(2Mr_H)$ is the rotation frequency of the BH and $r_H = r_g(1 + [1 - (a/M)^2]^{1/2})$ is the

radius of the SMBH horizon for angular momentum $J = aGM/c$; quantitatively, β drops by a factor of 177 from $a/M = 0.998$ to $a/M = 0.60$ using this fitting formula. We assume $a/M = 0.998$ to be the maximal possible SMBH spin (Thorne 1974) and $a/M = 0.60$ roughly corresponds to the SMBH spin without significant gas accretion (Volonteri et al. 2005; V05 hereafter). Hawley & Krolik (2006) also provide a different fitting formula, $\beta(a/M) = 0.002(1 - a/M)^{-1}$. Note that the Bardeen-Petterson (1975) effect likely aligns the spin of the inner accretion gas with the spin of the SMBH. Thus, we consider the issue of inevitable mis-alignment between the large-scale gas angular momentum vector and the SMBH spin irrelevant to jet production efficiency at the benefit of ridding ourselves of one additional potential parameter, because the alignment time scale of the SMBH spin to large scale accretion disk is probably significantly shorter than the time scale for enough gas to be accreted via disk to reach a maximally spinning SMBH (e.g., Natarajan & Pringle 1998). A related consequence will be that the powerful radio jets are almost always perpendicular to the large-scale accretion disk or perhaps the galactic plane.

2.3. Hot Accretion in “Dormant” SMBHs

For the majority of time, a SMBH may be “dormant”, i.e., inactive. Therefore, an estimate of the hot accretion in dormant SMBHs is useful. To do this, we need first to place the physical processes on SMBH scales in the context of galaxy formation, by beginning the discussion on galactic scales. In the standard cold dark matter model (Spergel et al. 2006) structures grow largely by mergers and accretion (e.g., Lacey & Cole 1993, LC hereafter). Keres et al. (2005), based on detailed analyses of smoothed particle hydrodynamic (SPH) simulations, have made an important discovery that there are two gas accretion modes on galactic scales, where massive galaxies in halos $\geq 10^{12} M_{\odot}$ accrete predominantly hot diffuse gas, whereas lower mass galaxies accrete progressively more cold gas. Birnboim &

Dekel (2003; Dekel & Birnboim 2006) provided a plausible physical explanation for this phenomenon, proposing that in large halos the cooling time of gas in the post-shock region is longer than the gas compression time scale and hence shocked gas is unable to cool, resulting in hot gas. Given that, we would like to ask a somewhat different question: how does a massive halo maintain a hot quasi-spherical gaseous atmosphere?

A gaseous atmosphere around a galaxy-size dark matter halo may be subject to thermal and Jeans instabilities. If we start with a just virialized halo with a hot atmosphere, the gas cloud is, by definition, (marginally) Jeans stable. Therefore, perturbations that are most susceptible to gravitational fragmentation are the largest possible ones of wavelength $\lambda = 2r$, at radius r . We will assume that some heating processes effectively transmit energy to potentially counter cooling at a speed close to the sound speed, which will be the case if dissipation is through acoustic waves or low Mach number weak shocks. Then, the non-fragmentation condition is: $t_{cool}/t_{sc} > 1$, where t_{cool} is the cooling time and $t_{sc} \equiv 2r/c_s$ the sound crossing time at r (c_s is the local sound speed). Figure 4 shows t_{cool}/t_{sc} as a function of radius for halos of different masses.

The existence of a critical halo mass, $M_d \sim 10^{12} M_\odot$, is evident from Figure 4. For halos more massive than M_d , $t_{cool}/t_{sc} > 1$ at all radii, indicating that gas at all radii is stable to fragmentation and the whole hot atmosphere remains quasi-spherical (at the virial temperature). As a result, subsequent infalling gas clouds may be shock heated and ram-pressure removed from their host dark matter halos, giving rise to “hot” accretion. But, even with the non-fragmentation condition met, some energy heating sources are still required in order to maintain the hot atmosphere in a quasi-steady state. For halos with $M \geq M_d$, heating due to gravitational energy released by accreting satellite halos/galaxies may keep the gas roughly at the virial temperature, as shown by direct high resolution simulations (Naab et al. 2006). Additional heating, such as feedback from star and/or

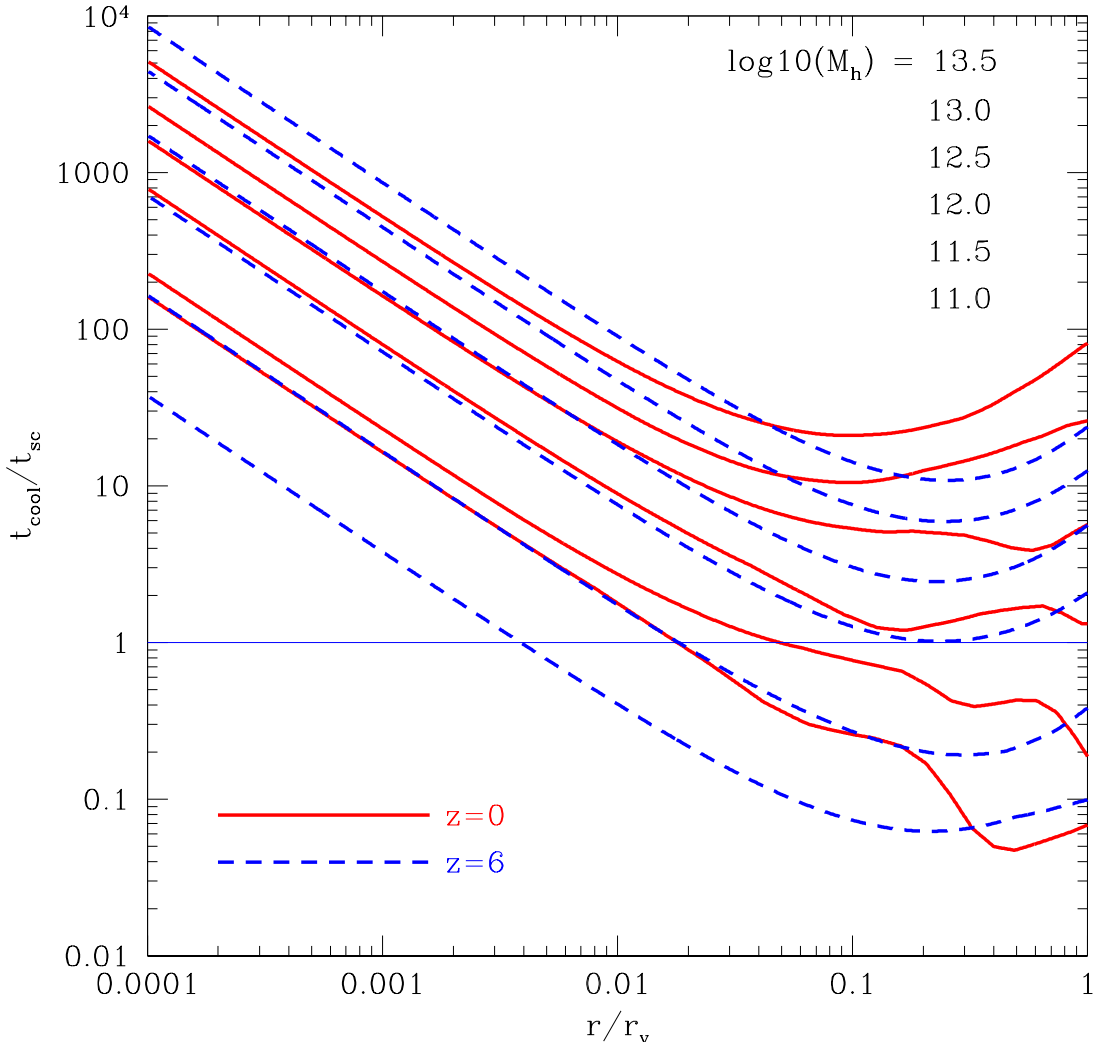


Fig. 4.— shows the ratio of cooling time to sound crossing time as a function of radius for galaxies of different masses at redshift $z = 6$ (dashed curves) and $z = 0$ (solid curves); r_v is the virial radius. We use the NFW halo density profile (Navarro, Frenk, & White 1997) (top curves at small radii) with halo concentration parameter as a function of halo mass and redshift taken from Dolag et al. (2004) based on simulations. (using a different, Moore et al. (1998) density profile hardly reaches a different conclusion). We use the Komatsu and Seljak (2001) method to compute the gas density and temperature profiles, where the ratio of the gas density to total density at large radii is normalized to the global ratio. A metallicity of $0.3 Z_\odot$ is used for the halo gas and the cooling functions are taken from Sutherland & Dopita (1993).

SMBH formation, may also play an important role. In the absence of any heating source, the hot atmosphere will contract in the gravitational potential well. However, since the non-fragmentation condition is met, the contraction may be able to maintain the original density profile.

For halos below M_d there is a radial range where the gas cloud has cooling time that is sufficiently short to cause it to fragment and a quasi-steady coherent hot gas cloud at virial temperature at the fiducial gas density may not be maintained. Consequently, the amount of hot gas may be reduced until the remaining hot, more rarefied atmosphere satisfies the non-fragmentation condition. Gas accretion will thus progressively become more dominated by cold accretion in halos less massive than M_d due to a thinner atmosphere. Figure 5 shows the relative reduction of hot gas density with respect to the fiducial case where the ratio of the gas density to total density at large radii is normalized to the global ratio; we have assumed for simplicity that the shape of the gas density profile remains unchanged. Taking the reduced hot gas density profile, as shown in Figure 5, we can estimate the QS-Bondi accretion rate onto the SMBH in dormant state, which is shown as the dotted curve in Figure 3. Note that this is only suggestive, since the overall atmosphere is subject to many other effects and likely dynamical.

The results based on this very simple analysis are broadly consistent with simulations of Cox et al. (2004) and Keres et al. (2005), who find that gas infall is almost all cold at $M_h \leq 10^{11} M_\odot$, with the fraction of cold accretion dropping to $\sim 50\%$ at $M_h \sim 3 \times 10^{11} M_\odot$, to nearly zero at $M_h \sim 10^{12} M_\odot$. The assumed zero metallicity in Keres et al. (2005) may have underestimated M_d by a factor of about two (Cattaneo et al. 2006), which would render a somewhat still better agreement between simulations and our simple model. It should be stressed that, while our simple physical picture intends to capture the essence of the primary physics, it is clearly incapable of accounting for all complexities in real

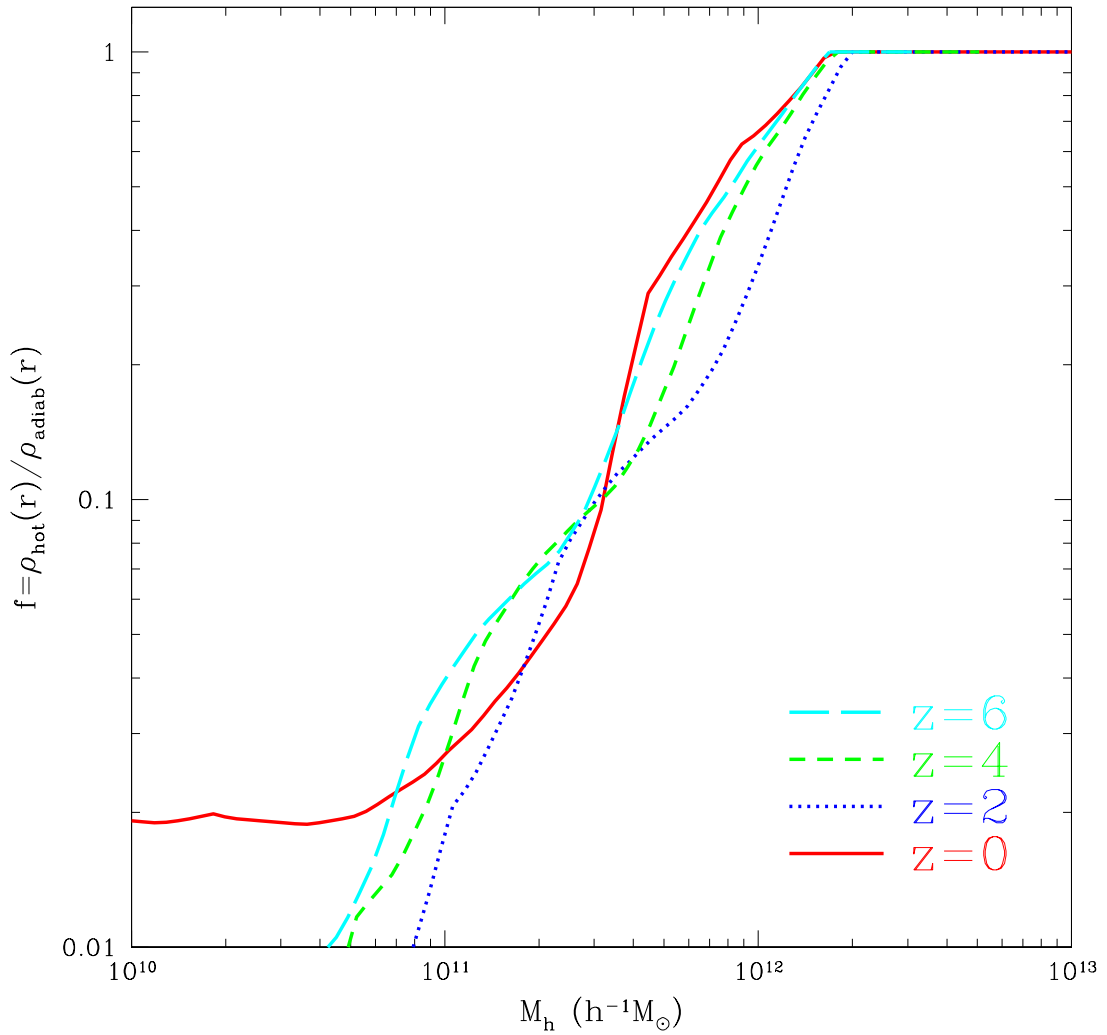


Fig. 5.— shows the relative reduction of gas density with respect to the fiducial case as a function of halo mass, assuming that the shape of the gas density profile remains unchanged, for redshift $z = (0, 2, 4, 6)$ with solid, dotted, dashed and long-dashed curves, respectively.

situations. For example, the merger/accretion processes are often anisotropic with a large fraction of activities (mass and energy flows) occurring along quasi-linear structures (filaments) that bridge dense lumps (Keres et al. 2005). But, for our purpose, it provides us with a simple quantitative way to represent the “outer boundary” and initial conditions for physical processes on smaller, SMBH scales, insofar as it fits direct simulations reasonably well. As a side note, it is interesting that M_d remains little changed at $z = 6$ compared to at $z = 0$. Several competing factors contribute to this weak evolution while higher density at higher redshift gives shorter dynamical time [$\propto (1+z)^{-3/2}$] and still shorter cooling time [$\propto (1+z)^{-3}$], lower concentrations of halos and a fixed halo mass corresponding to a higher virial temperature at higher redshift reduce the cooling time fortuitously by a compensatory factor.

It is useful to clarify an apparent inconsistency here. A flat rotation curve in the radial range $r > r_B$ may be a very good approximation (Sofue & Rubin 2001; Gavazzi et al. 2007). Thus, the gas density profile there may be relatively steep, possibly in the range r^{-1} to r^{-2} , as the solution to Equation (5) in §2.1 seems to suggest. But here (Figure 4) we show that the same ratio increases with decreasing radius. The difference is that, in the “dormant” state, the gas density profile has a flat profile at the center (“core”), while, in an “elevated” state, the central *total* gas density profile may be closer to an isothermal profile (e.g., Cen 2006), although the slope of the hot component becomes progressively shallower with increasing total accretion rate.

2.4. What Triggers Powerful Radio Activities?

We now consider how a dormant SMBH may be triggered to become active. We will advocate the mechanism proposed by Barnes & Hernquist (1991) & Mihos & Hernquist (1996) that significant galaxy mergers drive gas inward to fuel the central SMBHs, which in

some cases may trigger powerful jets, as we argue below. That powerful radio sources may be triggered by major mergers was pointed out long ago by Heckman et al. (1986), based on observational evidence.

We will adopt some of the elements in V05 on how the evolution of SMBH spins is governed by mergers of SMBHs and gas accretion in the context of hierarchical structure formation. In the absence of gas accretion but in the presence of SMBH mergers, the spins of SMBHs roughly retain the value given at birth, which, as in V05, is assumed to be ~ 0.60 and be the typical spin of each SMBH prior to a major merger. This means that elliptical galaxies, once formed, have just been eating up mostly smaller galaxies with their central SMBHs swallowing up smaller SMBHs randomly, which decreases a/M , if the initial spin is high. In other words, most elliptical galaxies get “reset” to a moderate spin during the long relatively “quiet” phases, if the initial spin is high, because they just enjoy a lot of minor mergers that spin it down but not significant gas accretion that would spin it up. As V05 have shown, major binary mergers of SMBHs with mass ratio q greater than 0.125 tend to produce faster spinning SMBHs, while less major mergers typically spin down SMBHs. Gas accretion is very effective to spin up a SMBH: a maximally rotating state ($a/M = 1$) is reached when the final SMBH mass is equal to $\sqrt{6}$ times the original SMBH mass (Bardeen 1970), i.e., roughly one e-folding, starting with a Schwarzschild SMBH. But, in the following, we intend to make some general statement without adhering to a specific model, such as in V05 where the amount of accreted gas for each major merger event is tightly pegged to the bulge rotation velocity (Volonteri, Haardt, & Madau 2003). In general, there may be four possible outcomes from significant mergers with respect to radio emission:

- (1) A relatively low-strength major merger does not produce maximally spinning SMBHs, even with both the binary SMBH coalescence and disk gas accretion, thus resulting

in a RQ AGN during its entire (limited) accretion history. While it is very uncertain, we tentatively denote mergers with $q = 0.1 - 0.5$ for this class and call them “significant mergers”.

(2) The binary SMBHs coalesce relatively early in the major merger event ($q \geq 0.5$) and that significantly increases the spin of the remnant SMBH. Then, continuous gas accretion causes the SMBH to maximally spin at a certain time. Subsequently, the AGN becomes radio-loud. In this case, an initial RQ AGN phase may precede the RL phase.

(3) A major merger ($q \geq 0.5$) drives disk gas accretion to gradually spin up the SMBH. Then, at a later time (when the disk gas accretion is still active) the binary SMBHs coalesce to cause the remnant SMBH to “switch” to the maximal spin. Subsequently, the AGN becomes radio-loud. In this case, an initial RQ AGN phase may also precede the RL phase.

(4) A major merger drives gas accretion to spin up the SMBH until the maximum spin. But the binary SMBHs are unable to coalesce during the entire active phase. In this case, an initial RQ AGN phase may again precede the RL phase. The possibility of having three separate cases (2-4) is due to the still uncertain time it takes for two SMBHs to merge. But in all three cases, the triggers are truly “major mergers”.

In our picture, RQ AGNs may be due to either a significant merger (Case 1) or the first phase of a major merger (Cases 2-4). But, since the frequency of merger events decreases sharply with increasing merger strength (i.e., mass ratio) (e.g., LC), we expect that RQ AGNs are likely to be predominantly contributed by Case (1). On the other hand, RL AGNs may be predominantly in the latter stage of the AGN event when the SMBH mass has roughly increased by one e-folding (Cases 2-4).

3. Some Observational Tests and Predictions

3.1. Strong Dependence of Maximum Jet Power on Black Hole Mass

Equation (7) and Figure 3 combine to yield the *maximum* strength of radio jets that is a strong function of M , shown in Figure 6 for a Kerr BH with $a/M = 0.998$ (red curves) and $a/M = 0.60$ (blue curves), respectively, using the fitting formula for $\beta(a/M)$ from McKinney (2005). Because \dot{m}_{QS} is expected to be non-zero for any SMBH, even in “dormant” state (the dotted and long-dashed curves in Figure 5), radio jets should emerge near SMBHs of all galaxies, as supported by recent observations (Ho 1999; Ulvestad et al. 1999; Kukula et al. 1999; Ulvestad & Ho 2001; Nagar, Wilson, & Falcke 2001; Giovannini et al. 2001; Bicknell 2002; Mundell et al. 2003; Falcke, Kording, & Nagar 2004; Anderson, Ulvestad, & Ho 2004; Gallimore & Beswick 2004; Nagar, Falcke, & Wilson 2005; Filho, Barthel, & Ho 2006; Gallimore et al. 2006).

However, the strength (and probably scale) of radio jets varies vastly, seen in Figure 5. For example, for low mass SMBHs ($\leq 10^6 M_\odot$), the *maximum* radio power is predicted to be low, in the range of $\sim 10^{36} - 10^{39}$ erg/s, in agreement with observations (e.g., Greene, Ho & Ulvestad 2006). Seyfert galaxies, having low M SMBHs, should not display powerful jets, as known (e.g., Lal, Shastri, & Gabuzda 2004). At the high end $M \geq 10^{8.5} - 10^{10} M_\odot$, radio jets could reach a maximum power in the range of $10^{44.5} - 10^{47.5}$ erg/s *for a nearly maximally rotating Kerr BH*, fully consistent with observed radio jets (Fanaroff & Riley 1974; Laing, Riley, & Longair 1983; Wall & Peacock 1985; Spinrad et al. 1985; McCarthy 1995). The maximum radio power roughly scales as M^2 (indicated by the dot-long-dashed line in Figure 6), a very steep dependence on M that is in fact in good agreement with observations (Ledlow & Owen 1996; Laor 2000; Lacy et al. 2001; Borošon 2002; Jarvis & McLure 2002, McLure & Jarvis 2004; Metcalf & Magliochetti 2005; Best et al. 2005). We find that, with the adopted $\beta(0.998)$, the following formula provides a good fit for the

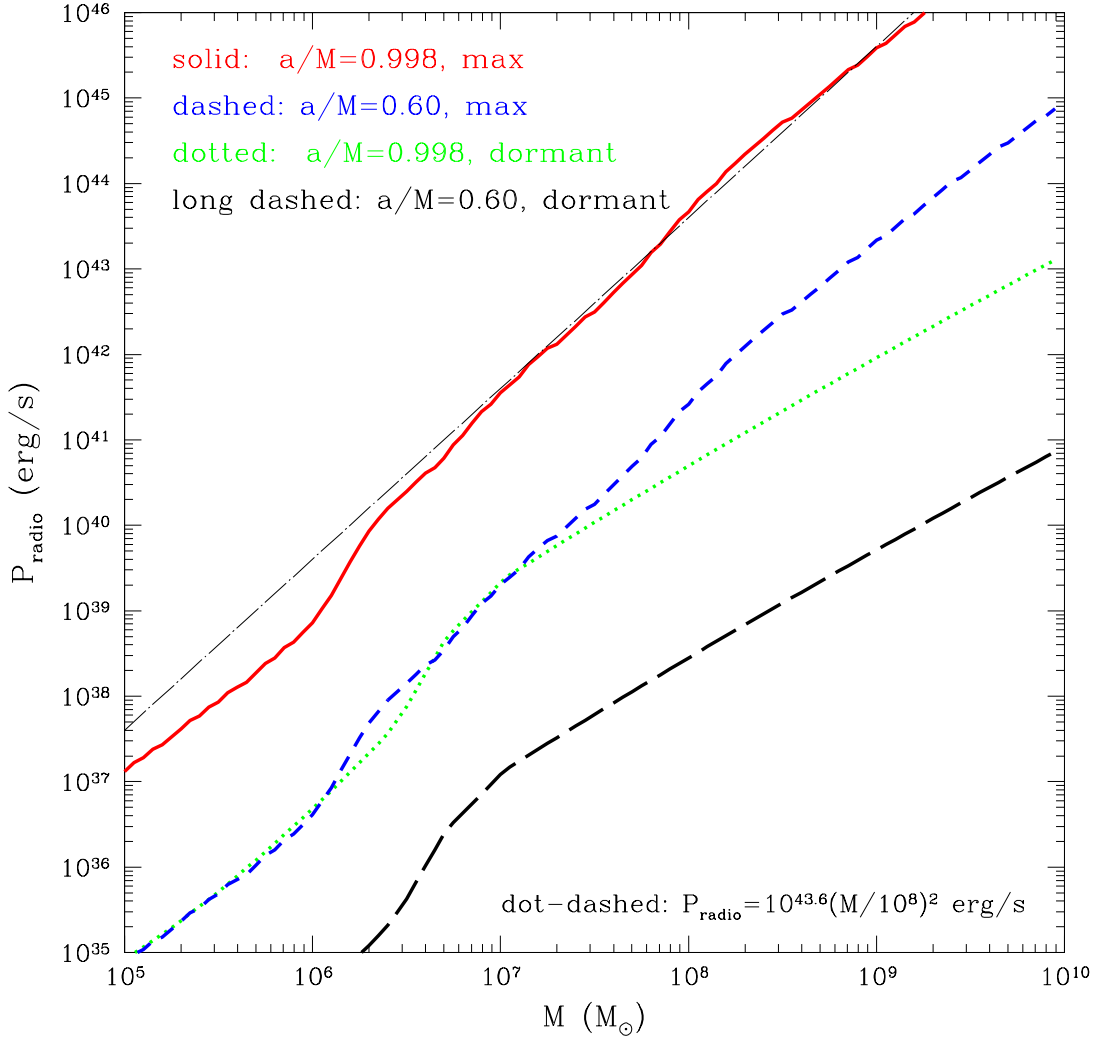


Fig. 6.— shows the maximum radio jet power as a function of M for SMBHs for two cases with $a/M = 0.998$ (solid curve) and $a/M = 0.50$ (dashed curve), respectively. Also shown as dotted and long dashed curves are the counterparts with a fiducial gas density profile, i.e., in a “dormant” state. The dot-long-dashed curve indicates $P_{\text{radio}} = 10^{43.6} (M/10^8 \text{ M}_\odot)^2 \text{ erg/s}$.

maximum jet power as a function of M :

$$\dot{P}_{radio} = 10^{43.6} \left(\frac{M}{10^8 M_\odot} \right)^2 \text{erg/s}, \quad (8)$$

shown as dot-long-dashed line in Figure 6. However, given the uncertainties with respect to both β and $\dot{m}_{QS,max}$, Equation (8) might be accurate only to an order of magnitude.

Finally, we show the corresponding radio power from SMBHs in dormant state in Figure 6 as the dotted and long-dashed curves, respectively, for $a/M = 0.998$ and $a/M = 0.60$. We see that, even in “dormant” state, a substantial radio power ($> 10^{39} \text{erg/s}$) from the nucleus should be expected for SMBHs with $M \geq 10^9 M_\odot$, while for low $M \leq 10^6 M_\odot$ SMBHs the radio power is expected to be smaller than $\sim 10^{36} \text{erg/s}$.

3.2. Evolution of Radio-Loud AGN Fraction with Redshift

Our scenario suggests that the RQ AGNs may be predominantly produced by significant mergers that have lower strengths than major mergers that result in RL AGNs. This property may be manifested in the evolution of the relative fractions of the RL and RQ AGNs, because the distribution of merger strength with redshift may be precisely predicted in the CDM model and is expected to evolve. We estimate this using the Extended Press-Schechter (EPS) theory (Bond et al. 1991; Bower 1991; LC). We use the instantaneous merger rate for a halo of mass M_p to merger with a halo of mass $\Delta M = M_f - M_p$ to form a halo of mass M_f (LC):

$$R_N(M_p \rightarrow M_f) dM_f = \sqrt{\frac{2}{\pi}} \frac{d\delta_c}{dt} \frac{d\sigma_f}{dM_f} \frac{1}{\sigma_f^2} \frac{1}{(1 - \sigma_f^2/\sigma_p^2)^{3/2}} \exp \left[-\frac{\delta_c(t)^2}{2} \left(\frac{1}{\sigma_f^2} - \frac{1}{\sigma_p^2} \right) \right] dM_f, \quad (9)$$

where σ_f and σ_p are the density variances of a sphere in the linear density field extrapolated to $z = 0$ that contains mass M_f and M_p , respectively; $\delta_c(t)$ is the critical density for collapse (equation 2.1 of LC); t is age of the universe at the epoch examined.

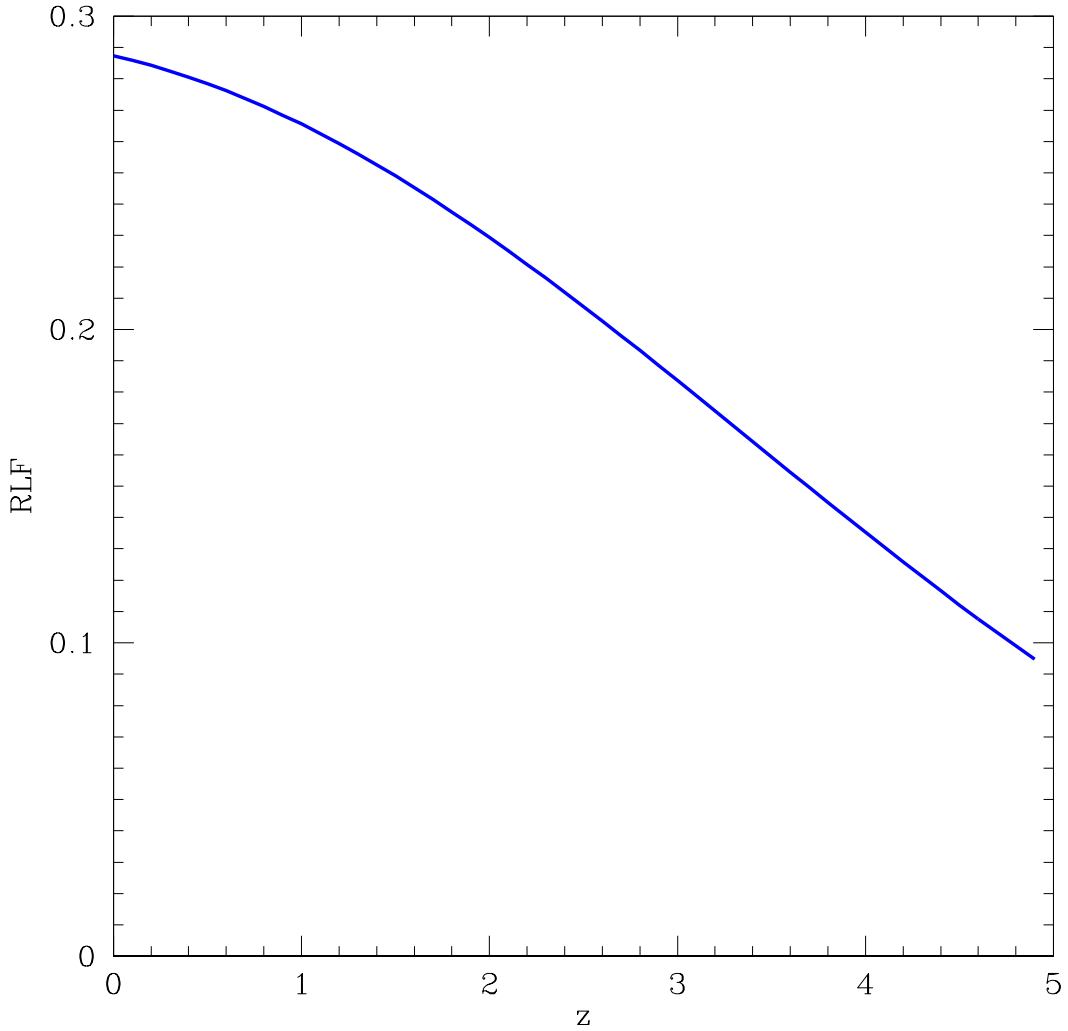


Fig. 7.— shows the ratio of merger rate with mass ratio $q \geq 0.5$ to those with $q \geq 0.1$ for a halo mass of $5 \times 10^{12} M_{\odot}$. The standard WMAP3-normalized cold dark matter model (Spergel et al. 2006) is used: $\Omega_M = 0.26$, $\Lambda = 0.74$, $H_0 = 72 \text{ km/s/Mpc}$, $n_s = 0.95$ and $\sigma_8 = 0.77$.

In the absence of more quantitative understanding of the physics of gas accretion and radio emission and their dependences on merger strength and SMBH mass, among others, it is uncertain to compute the dependence of RL fraction (RLF; Jiang et al. 2006) of quasars on the mass/luminosity of galaxies. For this reason, we will only compute the redshift evolution of the relative rates of mergers of different strengths at a fixed halo mass, hoping that there is little evolution in accretion processes at a fixed SMBH mass and merger strength. Figure 7 shows the ratio of merger rate with mass ratio $q \geq 0.5$ to those with $q \geq 0.1$ for a halo mass of $5 \times 10^{12} M_{\odot}$. If we use this ratio as a proxy for the RLF, we find that RLF of quasars is a decreasing function of increasing redshift, a trend that is in agreement with observations (Schmidt et al. 1995; Jiang et al. 2006). A good quantitative agreement between our model and observations may be obtainable, if one fine-tunes the mass ratio cutoffs for significant and major mergers.

3.3. Is There A Dichotomy in AGN Radio Loudness Distribution?

In our proposed picture there are two separate populations of AGNs. The RQ population that is primarily created by significant mergers likely substantially outnumbers the RL population that is triggered by more rare, major mergers. The peaks of the two populations may be well separated in radio loudness by, to the zero-th order, the ratio of $\beta(\text{loud})/\beta(\text{quiet})$, which may amount to $100 - 1000$, if we identify $\beta(\text{loud})$ with the case with maximal rotation and $\beta(\text{quiet})$ with the case with $a/M \sim 0.5 - 0.6$. There are, of course, a likely spread in a/M distributions. This is quite uncertain presently.

Thus, both scatters in optical luminosity at a fixed radio luminosity and in radio luminosities at a fixed optical luminosity would likely help smear out both peaks to some extent in the radio-loudness axis. More importantly, the sum of two decreasing monotonic functions of radio-loudness each spanning a range that is larger than the displacement of the

two functions in radio-loudness will likely largely produce a smooth overall distribution that suppresses or completely removes the secondary peak at the high radio-loudness. However, if one restricted oneself to an AGN sample where the range of SMBH mass is comparable to or narrower than the displacement between the RL and RQ population, then the secondary, smaller peak at the high radio-loudness may become visible.

We will use a simple toy model to illustrate this. Since the maximum radio jet power roughly scales as M^2 , then, if we assume that the optical luminosity scales as M (i.e., at a fixed disk accretion rate in Eddington units), the radio-loudness parameter R may be linearly proportional to M , albeit with a significant dispersion. Thus, we will adopt a standard Schechter function for the underlying radio-loudness distribution of the RQ population: $n_{RQ}(R)dR = A(R/R_*)^{-1.2} \exp(-R/R_*)dR$. The RL population is then assumed to bear the form: $n_{RL}(R) = 0.1n_{RQ}(R/\eta)$, where η is taken to be 200 [$\approx \beta(0.998)/\beta(0.6)$]. Observatioally, a cutoff in some apparent optical magnitude applied to a flux-limited sample essentially translates to a lower cutoff in M to both the RQ and RL populations. The corresponding lower radio-loudness cutoffs to the RQ and RL populations will be R_{cut} and ηR_{cut} , respectively. But the exact form at lower cutoff in R is uncertain and we will use simple functional forms $\exp(-(R_{cut}/R)^{1/2})$ and $\exp(-(\eta R_{cut}/R)^{1/2})$ for the RQ and RL populations, respectively, which multiply their respective $n(R)$ distributions. Figure 8 shows four cases with different R_{cut} . While we cannot ascertain the results precisely, the trend appears to be consistent with the observed trend found in White et al. (2007) in that a small secondary peak is visible in their full sample, which is then significantly enhanced when a high-redshift sub-sample is used. The reason is that taking only the high-redshift sub-sample may be effectively imposing a higher lower-limit on the SMBH mass. Similarly, the more prominent secondary peak found by Ivezic et al. (2002) may be a result of applying an optical magnitude cut ($i^* < 18.5$) to their SDSS sample of AGNs.

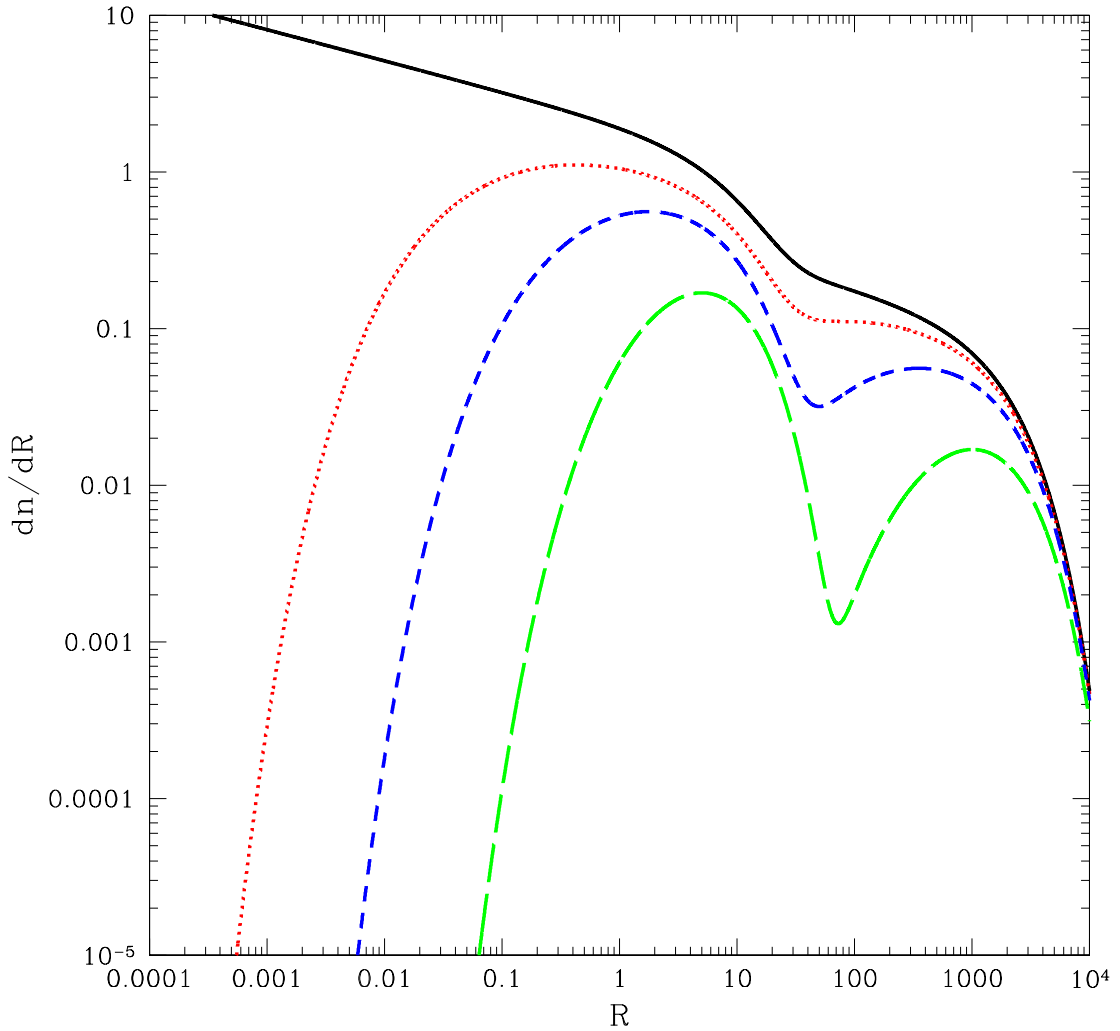


Fig. 8.— shows the radio loudness distributions for four cases with low cutoff equal to (1) no cutoff (solid), (2) $0.1R_*$ (dotted), (3) R_* (dashed) and (4) $10R_*$ (long-dashed).

Therefore, our conclusion is that, while there are truly two separate populations of AGNs, one RQ and the other RL with the overall shift in the radio-loudness possibly amounting to a factor of $100 - 1000$, a perfect AGN sample with an infinitely high observational sensitivity would in fact result in a radio-loudness distribution that is *not* bimodal. However, in an observational sample of AGNs with significant observational selection effects, primarily those which remove fainter optical objects, one may be able to unravel, incidentally, the two underlying populations in the form of a secondary peak at high radio-loudness. A definitive test of this picture may be obtained, for example, by applying the analysis of Ivezic et al. (2002) to a fainter optical cutoff, where the secondary peak should progressively shift to lower radio-loudness with a diminishing relative amplitude.

3.4. Some Additional Properties and Tests

Numerous other consequences and predictions may be made based on this general model. Here, we highlight several of them.

First, both RQ and RL quasars are expected to be drawn from the same underlying elliptical galaxy population, in agreement with observations (e.g., Bettoni et al. 2001; Scarpulla & Urry 2001; Kauffmann et al. 2003; Urry 2004). However, the average SMBH mass of RL quasars may be higher than that of RQ quasars by roughly one e-folding, consistent with observations (e.g., Corbin 1997; Laor 2000; Lacy et al. 2001; Boroson 2002; Jarvis & McLure 2002; Metcalf & Magliochetti 2005).

Second, since the hot accretion and cold disk accretion are practically “decoupled” in the sense that varying the hot accretion may not significantly alter the disk accretion physics, RQ and RL quasars should have nearly identical average IR-optical-UV properties which are assumed to be primarily due to the disk accretion, in agreement with observations

(e.g., Francis et al. 1993; Zheng et al. 1997).

Third, if each merger event that triggers an AGN phase is accompanied by a (central) starburst (e.g., Barnes & Hernquist 1991), the SN Ia rate may be higher in RL AGNs than in RQ AGNs. This is simply because RQ AGNs are formed by less major mergers (Case 1 in §2.4) and therefore they will experience less star formation hence fewer SN Ia’s. For Cases 2-4 the RL AGN phase may be delayed by roughly an e-folding or Salpeter time compared to the earlier RQ AGN phase. This delay time is shorter than the typical lifetime of progenitors of SN Ia supernovae of ~ 1 Gyr and hence the SN Ia rate is rising during the period, which would also result in RL AGN having higher SN Ia rate. Both scenarios thus yield a trend that appears to be supported by observations (e.g, Della Valle et al. 2005).

Fourth, under the assumption that more major mergers produce more pronounced central stellar “cores” in the final elliptical galaxy, carved out by the coalescence of the two central SMBHs (Faber et al. 1997; Milosavljevic et al. 2002), RL AGNs may preferentially be found in core elliptical galaxies. There is some observational indication that this may indeed be the case (de Ruiter et al. 2005; Capetti & Balmaverde 2006). If the other finding of Capetti & Balmaverde (2006), that RQ AGNs are found only in power-law galaxies, holds up, this suggests that RQ AGNs are primarily produced by significant mergers (Case 1 in §2.4), as expected in the standard cold dark matter model because mergers rate generally decreases rapidly with merger strength (mass ratio). The intriguing link between RL quasars and core elliptical galaxies may be indicative that massive binary SMBHs merge on a relatively short time scale, perhaps shorter than 10^8 yrs (e.g., Zier and Biermann 2001; Yu 2003; Escala et al. 2004).

Fifth, since the radio power is a strong function of M ($P_{jet} \propto M^2$), among radio-powerful AGNs there should be correlation between clustering strength and radio power *for radio-powerful AGNs*, in agreement with observations (e.g., Overzier et al. 2003), under the

assumption that more massive galaxies are more strongly clustered. However, some AGNs with very massive SMBHs may be RQ. As a result, for powerful AGNs (i.e., mostly above some high M threshold) radio-loud and RQ samples may exhibit comparable clustering strengths and inhabit similar environments, as indicated by observations (McLure & Dunlop 2001). On the other hand, spatial clustering of a random set of RQ AGNs would be an “average” over all SMBH masses. As such, it is “diluted” and should in general be less strongly clustered than that of powerful RL AGNs, in agreement with observations (e.g., Cress et al. 1996; Hall et al. 2001; Magliocchetti et al. 2004; Brand et al. 2005; Zheng et al. 2006; Bornancini et al. 2006).

Sixth, for Cases (2-4) (§2.4) it is possible sometimes that the cold disk accretion becomes diminished at some later stage, when the spin of the SMBH has become maximal and the hot accretion still remains vigorous. This may result in radio galaxies that do not have a significant amount of disk material, presumably including the purported obscuring torus. There are some observational indications for the existence of this type of objects (Whysong & Antonucci 2004; Muller et al. 2004; Kharb & Shastri 2004).

Seventh, in all Cases (1-4), at some later time the disk accretion may finally taper off. However, the hot accretion would gain in relative strength when total accretion or disk accretion decreases. By this time, on the order of a Gyr has elapsed since the onset of the merger event. We propose that this “trailing” AGN phase may be identified with Low-luminosity AGN (LLAGN) and LINERs (Low Ionization Narrow Emission-line Regions; Heckman 1980; Ho, Filippenko, & Sargent 2003). One specific prediction is that these objects are likely to be radio-loud, supported by observations (e.g., Ho 1999). More generally, there should be an anti-correlation between radio-loudness and disk accretion rate, in good agreement with observations (e.g., Oshlack, Webster, & Whiting 2001; Ho 2002). In addition, there may be a correlation between star formation activity and strength

of the AGN activities in these objects, since the later is on a declining slope because of declining accretion rate and the former declines with time because of passive aging.

Eighth, since major mergers, while rare, could occur multiple times in a Hubble time for some galaxies, restarting of radio jets may thus be expected, and observations support this expectation (e.g., Lara et al. 1999; Marecki et al. 2006). Because accretion disks from multiple mergers are generally not expected to be aligned, complex radio galaxy structures may be produced (e.g., Hogbom & Carlson 1974; Ekers et al. 1978; Leahy & Parma 1992; Merritt & Ekers 2002; Dennett-Thorpe et al. 2002; Gopal-Krishna, Biermann, & Wiita 2003).

3.5. A Thought on Radio Jet Feedback Effect

The problem of the jet feedback is unsolved. However, if we take the cue from the sizes of powerful radio jets (FR Is and FR IIs) (e.g., Urry & Padovani 1995), which often reach 100kpc-1Mpc, we may find some hint. At 100kpc for a medium of sound speed of 300km/s, the sound crossing time is $\sim 3 \times 10^8$ yrs. If most of the jet energy channels to and dissipates on these large-scales features, it means that the feedback of the jets on the surrounding gas will only be felt after this time scale. While this argument may be quite reasonable for powerful radio jets, one needs to be careful that the exact radial energy dissipation profile of jets on the surrounding medium is unknown. Furthermore, one might reason that less powerful jets in smaller SMBHs may start dissipating at smaller radii. But the countering effect that the surrounding gas medium will be proportionally less dense in less powerful jets, recalling that $P_{radio} \propto \dot{m}_{QS} \propto \rho_{hot}(r)$. As a result, it is unclear that jet feedback effect on less powerful jets may be more profound. As perhaps supportive evidence that the jets will be “slowed” down and dissipate by a denser medium at a more rapid rate is that the observed relic radio cavities in the cores of clusters of galaxies, where gas density is higher

than for example in regions surrounding isolated galaxies, are observed on a smaller scale of tens of kpc instead (e.g., McNamara et al. 2000, 2001; Fabian et al. 2000; Blanton et al. 2001). We will come back to examine this issue in much greater detail subsequently.

4. Conclusions

We suggest a co-existence of hot and cold accretion flows for any SMBH and propose that the hot accretion is a primary determinant of the radio emission from AGNs. Physically this is based on the notion that the external pressure provided by the hot accretion is required for collimating the radio jets. The spin of the SMBH also plays a major role in terms of the efficiency by which energy may be extracted in the form of radio jets from hot accretion. We propose that the jet power is directly proportional to the hot accretion rate and spin-dependent energy extraction efficiency in the form of jets (Equation 7).

A variety of predictions may be made and all seem to be in agreement with extant observations. Specifically,

- (1) Radio jets should emerge in all SMBH to varying strengths.
- (2) The maximum radio jet power increases with increasing SMBH mass approximately as M^2 .
- (3) While there are two separate underlying populations of RQ and RL AGNs, the apparently observed two peaks in the AGN radio loudness distribution are due to selection effect, caused by an imposed optical magnitude limit.
- (4) The RL fraction of quasars is expected to decrease with redshift in the cold dark matter model.
- (5) The host elliptical galaxies of RQ and RL quasars are drawn from the same

underlying elliptical galaxy population, although RL quasars are likely to possess SMBH that are somewhat more massive than their RQ counterparts and may reside predominantly in core elliptical galaxies.

(6) Low-luminosity AGN and LINERs may be the long, declining “trailing” phase following the initial, more luminous AGN phase. They should be RL and conform to the general, broad anti-correlation between radio-loudness and disk accretion rate. A correlation between star formation activity and strength of the AGN activities in these objects may be expected.

(7) RL galaxies may be expected to be more abundant in Type Ia supernovae.

(8) Among RL AGNs a correlation between radio power and clustering strength is predicted.

(9) Radio-quiet and RL AGNs should have nearly identical average IR-optical-UV properties.

I would like to thank especially Paul Wiita for many helpful discussions. I have also benefited from and am thankful for useful discussions with Martin Elvis, Jenny Greene, Luis Ho, Pat McCarthy, Jon McKinney, Dave Meier, Jerry Ostriker, Daniel Proga and Ari Socrates. I thank Michael Strauss for answering every observational question thrown his way. I thank Neta Bahcall, Jerry Ostriker, Alice Shapley and Michael Strauss for careful reading of the original, more broad manuscript. I am thankful to the hospitality of Observatories of Carnegie Institute of Washington during my visit in the summer of 2006, when I benefited from many discussions with local astronomers and the opportunity to give a colloquium partly on this subject. This research is supported in part by grants NAG5-13381, NNG05GK10G and AST-0507521.

REFERENCES

Allen, S.W., Dunn, R.J.H., Fabian, A.C., Taylor, G.B., & Reynolds, C.S. 2006, MNRAS, 372, 21

Anderson, J.M., Ulvestad, J.S., & Ho, L.C. 2004, ApJ, 603, 42

Antonucci, R. 1993, ARAA, 31, 473

Bahcall, N.A., Ostriker, J.P., Perlmutter, S., & Steinhardt, P. 1999, Science, 284, 1481

Bahcall, J.N., Kirhakos, S., Saxe, D.H., Schneider, D.P. 1997, ApJ, 479, 642

Balmaverde, B., & Capetti, A. 2005, A&A

Bardeen, J.M. 1970, Nature, 226, 64

Bardeen, J.M., & Petterson, J.A. 1975, ApJ, 195, L65

Barnes, J.E., & Hernquist, L. 1991, ApJ, 370, L65

Barthel, P.D. 1989, ApJ, 336, 606

Best, P.N., Kauffmann, G., Heckman, T.M., & Ivezic, Z. 2005, MNRAS, 362, 25

Bicknell, G.V. 2002, New Astronomy Rev. 46, 365

Blandford, R.D., & Begelman, M.C. 1999, MNRAS, 303, L1

Blandford, R.D., & Znajek, R.L. 1977, MNRAS, 179, 433

Blanton, E.L., Sarazin, C.L., McNamara, B.R., & Wise, M. 2001, ApJ, 558, L15

Blundell, K.M., & Rawlings, S. 2001, ApJ, 362, L5

Bond, J.R., Cole, S., Efstathiou, G., & Kaiser, N. 1991, ApJ, 379, 440

Bondi, H. 1952, MNRAS, 112, 195

Bornancini, C.G., Lambas, D.G., & De Breuck, C. 2006, MNRAS, 366, 1067

Boroson, T.A. 2002, ApJ, 565, 78

Bower, R.J. 1991, MNRAS, 248, 332

Brand, K., Rawlings, S., Hill, G.J., & Tufts, J.R. 2005, MNRAS, 357, 1231

Capetti, A., & Balmaverde, B., 2006, A&A, 453, 27

Casse, F., & Keppens, R. 2004, ApJ, 601, 90

Cattaneo, A., Dekel, A., Devriendt, J., Guiderdoni, B., & Blaizot, J. 2006, MNRAS, 370, 1651

Chakrabarti, S.K., & Titarchuk, L.G. 1995, ApJ, 455, 623

Corbin, M.R. 1997, ApJS, 113, 245

Cox, T.J., Primack, J., Jonsson, P., Somerville, R.S. 2004, ApJ, 607, L87

Cress, C.M., Helfand, D.J., Becker, R.H., Gregg, M.D., & White, R.L. 1996, in Clusters; lensing; and the future of the universe, ASP Conference Proceedings, Vol. 88, ed. V. Trimble and A. Reisenegger, p.193

Dekel, A., & Birnboim, Y. 2006, MNRAS, 368, 2

Dennett-Thorpe, J., Scheuer, P.A.G., Laing, R.A., Bridle, A.H., Pooley, G.G., & Reich, W. 2002, MNRAS, 330, 609

de Ruiter, H.R., Parma, P., Capetti, A., Fanti, R., Morganti, R., & Santantonio, L. 2005, A&A, 439, 487

De Villiers, J., Hawley, J.F., Krolik, J.H., & Hirose, S. 2005, ApJ, 620, 878

Dolag, K., et al. 2004, A& A, 416, 853

Eichler, D. 1993, ApJ, 419, 111

Ekers, R.D., Fanti, R., Lari, C., & Parma, P. 1978, Nature, 276, 588

Escala, A., Larson, R.B., Coppi, P.S., & Mardones, D. 2004, ApJ, 607, 765

Elvis, M. 2000, ApJ, 545, 63

Faber, S.M., et al. 1997, AJ, 114, 1771

Fabian, A.C., et al. 2000, MNRAS, 318, L65

Falcke, H., Krding, E., & Nagar, N.M. 2004, NewA, 48, 1157

Fanaroff, B.L., & Riley, J.M. 1974, MNRAS, 167, 31

Ferrarese, L., & Merritt, D. 2000, ApJ, 539, L9

Filho, M.E., Barthel, P.D., & Ho, L.C. 2006, A&A, 451, 71

Francis, P.J., Hooper, E.J., & Impey, C.D. 1993, AJ, 106, 417

Gallimore, J.F., & Beswick, R. 2004, AJ, 127, 239

Gallimore, J.F., Axon, D.J., O'Dea, C.P., Baum, S A., & Pedlar, A. 2006, AJ, 132, 546

Gavazzi, R., et al. 2007, astro-ph/0701589

Gebhardt, K., et al. 2000, ApJ, 539, L13

Giovannini, et al. 2001, ApJ, 552, 508

Gopal-Krishna, Biermann, P.L., & Wiita, P.J. 2003, ApJ, 594, L103

Greene, Ho, & Ulvestad 2006, ApJ, 636, 56

Heckman, T. 1980, A&A, 87, 152

Haehnelt, M., Natarajan, P., & Rees, M.J. 1998, MNRAS, 300, 817

Hall, P.B., et al. 2001, AJ, 121, 1840

Hawley, J.F., & Krolik, J.H. 2006, ApJ, 641, 103

Ho, L.C 1999, ApJ, 510, 631

Ho, L.C 2002, ApJ, 564, 120

Ho, L.C. 2005, ApJ, 629, 680

Ho, L.C., Filippenko, A.V., Sargent, W.L.W 2003, 583, 159

Hogbom, J.A., & Carlson, I. 1974, A&A, 34, 341

Ichimaru, S. 1977, ApJ, 214, 840

Ivezic, Z., et al. 2002, AJ, 124, 2364

Jarvis, M.J., & McLure, R.J, 2002, MNRAS, 336, L38

Jiang, L., et al. 2006, astro-ph/0611453

Kato, S., Fukue, J., Mineshige, S. 1998, in Black-hole accretion disks, ed. S. Kato, J. Fukue & S. Mineshige (Kyoto: Kyoto University Press)

Kauffmann, G., & Haehnelt, M. 2000, MNRAS, 311, 576

Kauffmann, G. et al. 2003, MNRAS, 346, 1055

Keres, D., Katz, N., Weinberg, D.H., & Dave, R. 2005, MNRAS, 363, 2

Kharb, P., & Shastri, P. 2004, A&A, 425, 825

Komatsu, E., & Seljak, U. 2001, MNRAS, 327, 1353

Krolik, J.H., Hawley, J.F., & Hirose, S. 2005, ApJ, 622, 1008

Kukula, M.J., Ghosh, T., Pedlar, A., & Schilizzi, R.T. 1999, ApJ, 518, 117

Lacey, C., & Cole, S. 1993, MNRAS, 262, 627

Laing, R.A., Riley, J.M., & Longair, M.S. 1983, MNRAS, 204, 151

Lal, D.V., Shastri, P., & Gabuzda, D.C. 2004, A&A, 425, 99

Laor, A. 2000, ApJ, 543, L111

Lara, L., et al. 1999, A&A, 348, 586

Leahy, J.P., & Parma, P. 1992, in Extragalactic Radio Sources: From Beams to Jets, ed., J. Roland, H. Sol, & G. Pelletier (Cambridge: Cambridge University Press), p307

Ledlow, M.J., & Owen, F.N. 1996, AJ, 112, 9

Ledlow, M.J., Owen, F.N., Yun, M.S., & Hill, J.M. 2001, ApJ, 552, 120

Lynden-Bell, D. 1996, MNRAS, 279, 389

Lynden-Bell, D. 2003, MNRAS, 341, 1360

Lynden-Bell, D. 2006, MNRAS, 369, 1167

McCarthy, P.J. 1995, ARAA, 31, 639

Magliocchetti, M., et al. 2004, MNRAS, 350, 1485

Magorrian, J., et al. 1998, AJ, 115, 2285

McNamara, B.R., et al. 2000, ApJ, 534, L135

McNamara, B.R., et al. 2001, ApJ, 562, L149

Marecki, A., Thomasson, P., Mack, K.-H., & Kunert-Bajraszewska, M. 2006, A&A, 448, 479

McKinney, J.C. 2005, ApJ, 630, L5

McLure, R.J., et al. 1999, MNRAS, 308, 377

McLure, R.J., & Dunlop, J.S. 2001, QSO hosts and their environments, ed. I. Marquez, et al. (Dordrecht: Kluwer Academic / Plenum Publishers), p27

McLure, R.J., & Jarvis, M.J. 2004, MNRAS, 353, L45

Merritt, D., & Ekers, R.D. 2002, Science, 297, 1310

Merritt, D., & Ferrarese, L. 2001, ApJ, 547, 140

Metcalf, R.B., & Magliocchetti, M. 2005, MNRAS, 365, 101

Mihos, C., & Hernquist, L. 1996

Milosavljevic, M., Merritt, D., Rest, A., van den Bosch, F.C. 2002, MNRAS, 331, L51

Miyoshi, M., Moran, J., Herrnstein, J., Greenhill, L., Nakai, N., Diamond, P., & Inoue, M. 1995, Nature, 373, 127

Moore, B., Governato, F., Quinn, T., Stadel, J., & Lake, G. 1998, ApJ, 499, L5

Muller, S.A.H., Haas, M., Siebenmorgen, R., Klaas, U., Meisenheimer, K., Chini, R., & Albrecht, M. 2004, A& A, 426, L29

Mundell, C.G., Wrobel, J.M., Pedlar, A., & Gallimore, J.F. 2003, ApJ, 583, 192

Naab, T., Johansson, P.H., Efstathiou, G., & Ostriker, J.P. 2005, astro-ph/0512235

Nagar, N.M., Falcke, H., & Wilson, A.S. 2005, A& A, 435, 521

Nagar, N.M., Wilson, A.S., & Falcke, H. 2005, ApJ, 559, L87

Narayan, R., & Yi, I. 1994, ApJ, 428, L13

Natarajan, P., & Pringle, J.E. 1998, ApJ, 506, L97

Navarro, J.F., Frenk, C.S., & White, S.D.M. 1997, ApJ, 490, 493

Okamoto, I. 1999, MNRAS, 307, 253

Overzier, R.A., Rttgering, H.J.A., Rengelink, R.B., & Wilman, R.J. 2003, A&A, 405, 53

Proga, D. 2005, ApJ, 629, 397

Proga, D., & Begelman, M.C. 2003, ApJ, 582, 69

Quataert, E., & Gruzinov, A. 2000, ApJ, 539, 809

Rees, M.J., Phinney, E.S., Begelman, M.C., & Blandford, R.D. 1982, Nature, 295, 17

Rees, M.J. 1984, ARAA, 22, 471

Richstone, D., et al. 1998, Nature, 395, A14

Scarpa, R., & Urry, C.M. 2001, ApJ, 556, 749

Schmidt, M., van Dokkum, J.H., Schneider, D.P., & Gunn, J.E. 1995, AJ, 109, 473

Shakura, N.I., & Sunyaev, R.A. 1973, A&A, 24, 337

Spergel, D.N., et al. 2006, astro-ph/0603449

Spinrad, H., Marr, J., Aguilar, L., & Djorgovski, S., PASP, 97, 932

Spruit, H.C., Foglizzo, T., & Stehle, R. 1997, MNRAS, 288, 333

Sutherland, R.S., & Dopita, M.A. 1993, ApJS, 88, 253

Thorne, K.S. 1974, ApJ, 191, 507

Tremaine, S., et al. 2002, ApJ, 574, 740

Ulvestad, J.S., & Ho, L.C. 2001, ApJ, 562, L133

Ulvestad, J.S., & Wilson, A.S. 1989, ApJ, 343, 659

Ulvestad, J.S., Wrobel, J.M., Roy, A.L., Wilson, A.S., Falcke, H., & Krichbaum, T.P. 1999, ApJ, 517, L81

Urry, M. 2004, AGN Physics with the Sloan Digital Sky Survey, ed. G.T. Richards and P.B. Hall, ASP Conference Series, Volume 311 (San Francisco: Astronomical Society of the Pacific), p49

Urry, C.M., & Padovani, P. 1995, PASP, 107, 803

Volonteri, M., Haardt, F. & Madau, P. 2003, ApJ, 582, 559 (V05)

Volonteri, M., Madau, P., Quataert, E., & Rees, M.J. 2005, ApJ, 620, 69

Wall, J.V., & Peacock, J.A. 1985, MNRAS, 216, 173

Wall, J.V., & Peacock, J.A. 1985, MNRAS, 216, 173

White, R.L., Helfand, D.J., Becker, R.H., Glikman, E., & de Vries, W. 2007, ApJ, 654, 99

Whysong, D., & Antonucci, R. 2004, ApJ, 602, 116

Yu, Q. 2002, MNRAS, 331, 935

Zheng, W., Kriss, G.A., Telfer, R.C., Grimes, J.P., & Davidsen, A.F. 1997, ApJ, 475, 469

Zheng, W., et al. 2006, ApJ, 640, 574

Zier, C., & Biermann, P.L. 2001, A&A, 377, 23